Available online at www.sciencedirect.com
ScienceDirect
Scripta Materialia 59 (2008) 356–359
Scripta MATERIALIA
www.elsevier.com/locate/scriptamat

Producing nanograined microstructure in Mg–Al–Zn alloy by two-step friction stir processing

C.I. Chang,[a] X.H. Du[a,b] and J.C. Huang[a,*]

[a] *Institute of Materials Science and Engineering, Center for Nanoscience and Nanotechnology, National Sun Yat-Sen University, Kaohsiung 804, Taiwan, ROC*
[b] *Department of Materials Engineering, Shenyang Institute of Aeronautical Engineering, Shenyang 110034, China*

Received 19 February 2008; revised 3 April 2008; accepted 3 April 2008
Available online 11 April 2008

Nanograined structures with an average grain size of ~85 nm have been achieved in solution hardened AZ31 magnesium alloy by two-pass friction stir processing under rapid heat sink in which the second pass has a lower heat input. The mean hardness of the nanograined region reaches ~1.5 GPa (or 150 H_v), about three times that of the matrix. The evolution of the nanograined structure is also investigated.

Keywords: Friction stir processing; Magnesium alloy; Nanograined microstructure; Microhardness

Numerous investigations have demonstrated the considerable advantages offered by the mechanical properties of ultrafine-grained (UFG) or nanostructured materials over conventional coarse-grained structures [1,2]. Therefore, to produce bulk nanograined structures in conventional engineering materials, such as Mg alloys, is of significant scientific and practical interest. Of the many techniques used for processing fine-grained materials directly in bulk form, severe plastic deformation (SPD), is considered to be the most promising process [3]. Thus, in the past decade, several SPD approaches [4], such as equal channel angular pressing (ECAP) [5], accumulative roll bonding (ARB) [6] and high-pressure torsion (HPT), have been applied to the grain refinement of bulk Mg alloys. It was found that twinning and dynamic recrystallization (DRX) were responsible for the grain refinement during these processes [4–9].

In addition to the conventional one-step process, Horita et al. [10] demonstrated a two-step processing route, designated EX-ECAP, in which the cast material is initially extruded and then processed using ECAP. EX-ECAP can produce finer grains than the use of only one extrusion or ECAP step. Matsubara et al. [11] and Lin et al. [12] also fabricated the UFG Mg alloys by two-step processing. The original coarse grain size can be reduced to less than 10 μm after extrusion at 300 °C and was further refined to around 0.7 μm after subsequent 8-pass ECAP at 200 °C [12]. However, in most cases, the grain size of the final structure is still in the micrometer or submicrometer range. Even for EX-ECAP, the resulting microstructure still cannot be refined to the nanoscale. Sun et al. [8] produced nanometer-sized grains in the surface layer of AZ91 magnesium alloy by surface mechanical attrition treatment (SMAT). After sufficient processing time, a thin nanometer-scale layer less than ~100 nm can be produced through DRX. However, it is only a thin surface layer and production of bulk nanomaterials remains difficult. Extra-fine grain sizes in the range of 30–180 nm have been demonstrated in Al alloys using reduced friction stir processing (FSP) with a fine sharp pin [13], but the same process has not yet been reported for Mg alloys. So far, all the production methods result in nanoscaled Mg materials restrained in a thin layer form or precipitate-hardened Mg alloys (such as AZ91).

FSP has been demonstrated to be an efficient new method of grain refinement [14–17], providing more intense plastic deformation as well as higher strain rates than other SPD methods. It was found that the UFG structure is more easily achieved in precipitate-hardened Mg alloys or Mg-based composites due to the effective pinning effect from the precipitates or ceramic particles on the grain boundaries [18–21]. Due to the rapid growth kinetics of single-phase grains it is difficult to

* Corresponding author. Tel.: +886 7 525 2000; fax: +886 7 525 4099; e-mail: jacobc@mail.nsysu.edu.tw

1359-6462/$ - see front matter © 2008 Acta Materialia Inc. Published by Elsevier Ltd. All rights reserved.
doi:10.1016/j.scriptamat.2008.04.003

achieve a UFG structure of pure Mg or solution hardened Mg alloys (such as AZ31) with a low content of alloying elements. Nevertheless, by using our newly developed FSP system equipped with efficient cooling apparatus, a UFG structure (mean grain size less than 300 nm) of AZ31 has been successfully prepared [22]. In order to achieve a nanomicrostructure, a two-step FSP is proposed. By tailoring the processing parameters, i.e., parameters and tool size, the heat input can be controlled.

The material for this study was commercial AZ31 Mg alloy with the chemical composition Mg–3.02Al–1.01Zn–0.30Mn (in mass%). The as-received billet (178 mm in diameter and 300 mm long) possessed nearly equiaxed grains of around 75 μm in size. In order to obtain rapid heat sink during FSP, an efficient cooling system was employed in this study. The liquid nitrogen cooling system has been described in a previous paper [22].

The two-pass FSP consisted of two different FSP parameters. The first pass was performed using a tool with a shoulder diameter, pin tool diameter and length of 10 mm, 3 mm and 3 mm, respectively. The second pass on the same place and along the same direction was performed with lower heat input by using a smaller tool with a shoulder diameter, pin tool diameter and length of 6 mm, 2 mm and 2 mm, respectively. For the second pass, the advancing direction was the same as the first-pass and the smaller pin tool could generate less friction heat. A rotation speed of 1000 rpm and a travel speed of 37 mm min^{-1} were applied for both passes. The tool rotation axis was tilted 1.5° to the workpiece surface.

Microstructural and hardness characterizations in this study are focused on the central and bottom parts of the nugget zone, where the cooling rate is the highest. The grain structures of processed specimens were examined by field emission scanning electron microscopy (SEM) and transmission electron microscopy (TEM). The TEM specimens were prepared by a focus ion beam system (SMI 3050 SE, Seiko). The grain size was measured by Optimas® image analysis software on the SEM micrographs. The Vickers hardness tests were conducted on the cross-sectional plane, using a Vickers indenter with a 200 gf load for 10 s.

Figure 1 shows two examples of TEM micrographs after the first FSP pass. In addition to the submicron fine grains, some microstructural defects such as dislocation walls and subgrains can also be observed in the first-pass samples. The initial 75 μm grain size in the as-received AZ31 billet has been effectively refined to ~270 nm on average (ranging from 100 to 500 nm) by a single FSP pass. Figure 2 presents some examples of typical microstructures observed in the two-pass FSP AZ31 alloy in the as-FSP condition, together with their selected area diffraction (SAD) patterns. The pattern exhibits scattered rings, indicating that there are many fine equiaxed grains with random misorientations in the selected regions. Figure 2c and d, shows that clearly nanosized grains have formed within highly deformed subgrains along the boundaries or the triple points of the recrystallized grains. This clean nanometer grain implies the elimination of strain even through there is still high strain in the surrounding area.

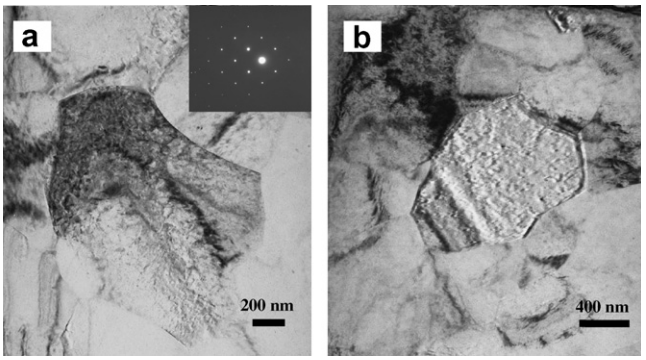

Figure 1. Typical TEM micrographs of the first-pass FSP AZ31 specimens, together with the selected area diffraction pattern.

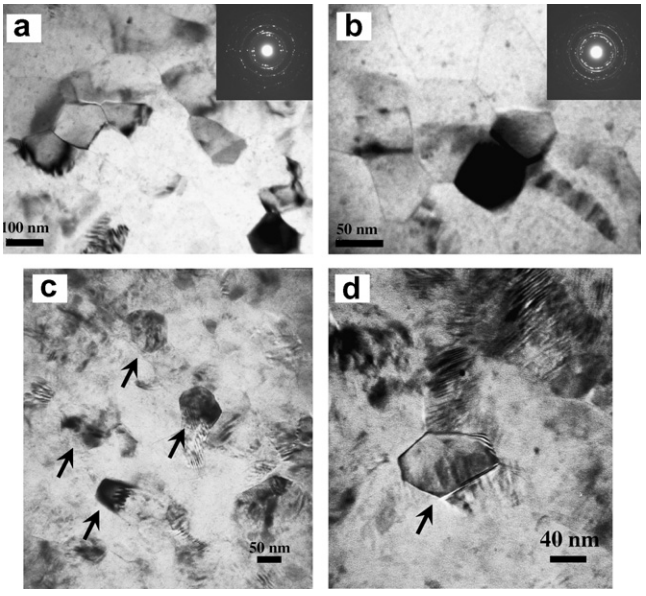

Figure 2. TEM micrographs of the two-pass FSP AZ31 specimens in the as-processed condition, together with the selected area diffraction patterns.

A typical SEM micrograph of the two-pass FSP AZ31 specimen is shown in Figure 3a. Figure 3b shows the grain size distribution of the two-pass FSP specimens, which is summarized from numerous SEM micrographs, demonstrating that the grains range from 20 to 200 nm with an average grain size of ~85 nm. Since the grains finer than 30 nm are difficult to resolve by field emission SEM, but are indeed observed by TEM, the

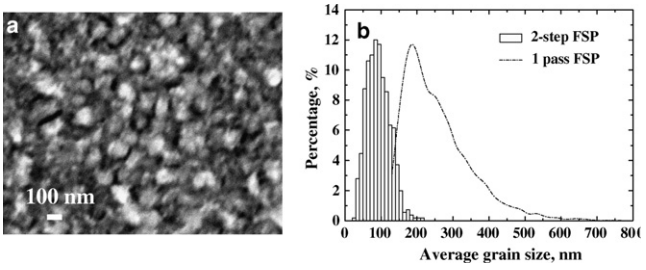

Figure 3. (a) Field emission SEM micrograph of the two-pass FSP AZ31 alloy and (b) grain size distribution charts of the nanocrystalline microstructure in the one-pass and two-pass FSP AZ31 specimens.

actual average grain size should be less than 85 nm. The previous size distribution of the one-step specimen is also included for comparison. It can be seen that the fine grains obtained from the first pass, around 270 nm in average and ranging from 100 to 500 nm, have been further refined to an average of 85 nm, ranging from 20 to 200 nm. The current UFG structure is finer than all grain structures achieved by previous two-step EX-ECAP and one-step FSP processes.

Note that the grain size distribution of the two-pass specimen does not exhibit apparent left skew behavior (i.e., few exceptionally large grains), as would be the case for grains that have grown to the coarsening or coalescence stage. The nearly normal distribution suggests that the nanograins in the two-pass specimen have been limited within the nucleation and early growth stages, avoiding coarsening and coalescence. On the other hand, the one-pass curve is still left skewed, with a few grains approaching 500–600 nm.

The degree of refinement and the extent of homogeneity of the final microstructure are two aspects that are most noticeable in the material prepared by the FSP process. These nanometer grains are also proved by microhardness tests. The measured hardness values after the first FSP pass are scattered within 1.13–1.25 GPa (or 115–128 in H_v scale), and after the second FSP pass are scattered within 1.27–1.52 GPa (or 130–155 in H_v scale), which is about three times the value of the AZ31 matrix, ~0.5 GPa (or 50 in H_v scale), indicating that the nanograined microstructure has strengthened significantly the AZ31 Mg alloy.

The one-pass FSP can therefore achieve UFG microstructure in AZ31 Mg alloy with an average grain size about 270 nm. The possibility of further grain refinement by the second pass can be evaluated by the relationship between the Zener–Hollomon parameter, Z, and the average recrystallized grain size, d, in μm. First, the strain rate and working temperature of the nugget region during FSP need to be determined. The material flow strain rate, $\dot{\varepsilon}$, during the second pass FSP may be estimated by torsion-type deformation as [15]: $\dot{\varepsilon} = R_m \cdot 2\pi\gamma_e/L_e$, where R_m is assumed to be about half of the pin rotational speed, namely 1000/2 rpm, and r_e and L_e are the effective (or average) radius and depth of the dynamically recrystallized zone. An effective radius, r_e, that can represent the average radius for all parts of the materials inside this zone, is assumed to equal about 0.78 (or $\pi/4$ [23]) of the observed zone boundary radius (1.17 mm in the current case). A similar argument can also be applied to L_e (~0.78 × 2 mm). Thus, $\dot{\varepsilon}$ can be calculated to be ~31 s^{-1}. The relationship between Z and d in μm for the AZ31 alloy during FSP can be traced by the equation established in the previous work [15]: $\ln d = 9.0 - 0.27 \ln Z$, where $Z = \dot{\varepsilon}\exp(Q/RT)$, Q is the activation energy for lattice diffusion (135 kJ mol^{-1} [24]) and RT has its usual meaning. In this case, with an average grain size of ~85 nm and a strain rate of ~31 s^{-1}, the working temperature can be calculated as ~143 °C. This means that if the working temperature can be controlled to as low as 143 °C (or even lower), the resulting grain size in the two-pass AZ31 FSP specimen can be refined to ~85 nm or less. In the present FSP case under effective rapid cooling and lower heat input during the second FSP pass, this condition appears to be fulfilled.

Under thermomechanical treatments, grain coarsening or grain refinement can occur concurrently during deformation. The grain size evolution is dependent on the initial grain size and deformation temperature. Takara et al. [25] recently proposed that the critical grain size, d_{crit} in μm, above which grain refinement would occur during deformation, could be given by the following empirical equation for the AZ31 alloy:

$$d_{crit} = 650Z^{-0.2} = 650\left\{\dot{\varepsilon} \times \exp\left(\frac{Q}{RT}\right)\right\}^{-0.2}, \quad (1)$$

Using a strain rate of 31 s^{-1} and an estimated working temperature of 143 °C, the critical grain size for further grain refining based on Eq. (1) will be about 133 nm, which is smaller than initial grain size (~270 nm) after the first FSP pass and before the second pass. Hence, for the present initial grain size, strain rate and working temperature, the grain refining process is capable of carrying on in the second FSP pass, as long as the low FSP heat input and rapid cooling is maintained for the AZ31 alloy.

From the grain evolution point of view, it is interesting to understand how the nanocrystalline structure is achieved during the two-pass FSP of AZ31 alloy. For most research reports on the recrystallization of the Mg alloy during thermomechanical treatments such as ECAP, rolling or extrusion, continuous DRX (CDRX) has been considered to account for the recrystallization and grain refinement [26,27]. The rapid diffusion rate of Mg alloys at elevated temperatures of 200–400 °C, as compared with the fine-grained Al counterparts [24,28–30], favor CDRX [27]. Meanwhile, during DRX, nuclei tend to form preferentially in regions where the local degree of deformation is highest, such as grain boundaries, deformation bands, inclusions, twin intersections and free surfaces. Due to the paucity of such "sites" for nucleation in the original coarse microstructure (~75 μm) of the first-pass FSP samples, more dislocation walls and even subgrain boundaries form to accommodate the high strain incompatibility. Therefore, CDRX may be responsible for the grain refinement from the original 75 μm to ~270 nm during the first FSP pass.

However, discontinuous DRX (DDRX) might be reasonable for the second FSP pass from ~270 nm down to ~85 nm. The difference between FSP and the previously reported SPD processes may lie in the strain rate. Wang et al. [31] have reported that the strain rate plays an important role in refining grains into the nanometer region during the SPD processes. The strain rates of ECAP and HPT are too low to induce enough twinning activity and to form nanometer grains. However, for the second pass FSP, the high strain rate will cause a complex stress state and result in strain components with very large strain gradients. Thus, large numbers of microstructural defects are introduced to accommodate the strain incompatibility, which is beneficial to discontinuous nucleation.

Thus, during the second FSP pass, the remaining high-density dislocation walls and subgrains as well as fine recrystallized grain boundaries can all become

"sites" for the nucleation of recrystallized grains. Then, under the high strain-rate FSP, DDRX may be dominant, which results in the formation of copious nuclei. This can be verified by the TEM observations of Figure 2c and d, which shows that copious nuclei have been formed in the highly strained regions, as denoted by the black arrows.

It should be mentioned that the DDRX process can significantly refine the grains, but the newly formed grains will be subject to growth and coarsening, which are controlled by volume diffusion under the condition of SPD. The working temperatures are crucial, especially for the clean solution hardened AZ31 alloy. However, in this current study, using a cooling system with liquid nitrogen, the heat generated from the input work can be conducted rapidly away by the effective heat sink. Thus, the recrystallized ultrafine grains can be maintained. In some places, the grain size has been refined to about 20 nm.

On the basis of microstructural observations, the evolution of the nanostructure can be described in three stages. (i) In the first FSP pass, micron- or submicron-scaled grains are introduced in the FSP-processed plate via CDRX. (ii) In the second FSP pass, copious nuclei form via DDRX due to the high strain rate and pre-existing microstructural defects. (iii) The growth of the recrystallized grains is limited due to the effective removal of heat via the liquid nitrogen cooling system. Figure 4 is a schematic diagram showing the procedures for evolution of the nanostructures via the recrystallization mechanism during two-pass FSP.

In summary, nanograined structure can be achieved in AZ31 Mg alloy through two-pass FSP combined with an efficient heat sink. The mean grain sizes can be refined to ~85 nm. The highest microhardness reaches 1.52 GPa (or 155 in H_v scale), which is about three times that of the AZ31 matrix. During the first FSP pass, highly strained regions as well as dislocation walls, subgrains and recrystallized grains are introduced, mainly via CDRX. During the second FSP pass, DDRX appears to be responsible, owing to the lower heat input, high total strain, high strain rate and copious sites for nucleation. This fundamental understanding of nanocrystalline evolution makes it possible to control the final microstructure, including grain size, grain boundary structure and dislocation density, by changing the processing parameters and cooling rate.

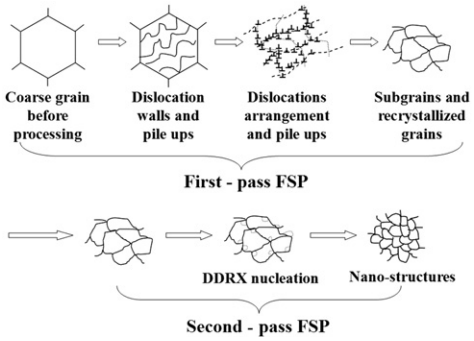

Figure 4. Schematic illustration of the grain refinement process of the two-pass FSP AZ31 Mg specimens.

The authors would like to gratefully acknowledge the sponsorship from the National Science Council of ROC under the project NSC 96-2628-E-110-008. The X.H.D. is grateful for postdoctoral sponsorship from the NSC under the contrast NSC 95-2816-E-110-001.

[1] C.C. Koch, D.G. Morris, K. Lu, A. Inoue, Mater. Res. Soc. Bull. 24 (1999) 54.
[2] S.X. McFadden, R.S. Mishra, R.Z. Valiev, A.P. Zhilyaev, A.K. Mukherjee, Nature 398 (1999) 684.
[3] T.C. Lowe, R.Z. Valiev (Eds.), Investigations and Applications of Severe Plastic Deformation, Kluwer, Dordrecht, 2000.
[4] R.Z. Valiev, R.K. Islamgaliev, I.V. Alexandrov, Prog. Mater. Sci. 45 (2000) 103.
[5] M. Mabuchi, K. Ameyama, H. Iwasaki, K. Higashi, Acta Mater. 47 (1999) 2047.
[6] M.T. Perez-Prado, J.A. del Valle, O.A. Ruano, Scripta Mater. 51 (2004) 1093.
[7] M.M. Myshlyaev, H.J. McQueen, A. Mwembela, E. Konopleva, Mater. Sci. Eng. A 337 (2002) 121.
[8] H.Q. Sun, Y.N. Shi, M.X. Zhang, K. Lu, Acta Mater. 55 (2007) 975.
[9] Q. Yang, A.K. Ghosh, Acta Mater. 54 (2006) 5147.
[10] Z. Horita, K. Matsubara, K. Makii, T.G. Langdon, Scripta Mater. 47 (2002) 255.
[11] K. Matsubara, Y. Miyahara, Z. Horita, T.G. Langdon, Acta Mater. 51 (2003) 3073.
[12] H.K. Lin, J.C. Huang, T.G. Langdon, Mater. Sci. Eng. A 402 (2005) 250.
[13] Y.J. Kwon, I. Shigematsu, N. Saito, Scripta Mater. 49 (2003) 785.
[14] R.S. Mishra, M.W. Mahoney, S.X. McFadden, N.A. Mara, A.K. Mukherjee, Scripta Mater. 42 (2000) 163.
[15] C.I. Chang, C.J. Lee, J.C. Huang, Scripta Mater. 51 (2004) 509.
[16] Y.S. Sato, Y. Kurihara, S.H.C. Park, H. Kokawa, N. Tsuji, Scripta Mater. 50 (2004) 57.
[17] J.Q. Su, T.W. Nelson, C.J. Sterling, Scripta Mater. 52 (2005) 135.
[18] Y. Morisada, H. Fujii, T. Nagaoka, M. Fukusumi, Scripta Mater. 55 (2006) 1067.
[19] C.J. Lee, J.C. Huang, P.J. Hsieh, Scripta Mater. 54 (2006) 1415.
[20] C.J. Lee, J.C. Huang, Mater. Trans. 47 (2006) 2773.
[21] C.I. Chang, Y.N. Wang, H.R. Pei, C.J. Lee, J.C. Huang, Mater. Trans. 47 (2006) 2942.
[22] C.I. Chang, X.H. Du, J.C. Huang, Scripta Mater. 57 (2007) 209.
[23] A.J. Ardell, Metall. Trans. 16A (1985) 2131.
[24] H.J. Forst, M.F. Ashby, Deformation–Mechanism Maps, Pergamon Press, Oxford, 1982, pp. 21 and 44.
[25] A. Takara, Y. Nishikawa, H. Watanabe, H. Somekawa, T. Mukai, K. Higashi, Mater. Trans. 45 (2004) 2377.
[26] K. Higashi, J. Wolfenstine, Mater. Lett. 10 (1991) 329.
[27] T. Mohri, M. Mabuchi, M. Nakamura, T. Asahina, H. Iwasaki, T. Aizawa, K. Higashi, Mater. Sci. Eng. A 290 (2000) 139.
[28] H.-P. Pu, F.C. Liu, J.C. Huang, Metall. Mater. Trans. A 26 (1995) 1153.
[29] J.C. Huang, I.C. Hsiao, T.D. Wang, B.Y. Lou, Scripta Mater. 43 (2000) 213.
[30] I.C. Hsiao, J.C. Huang, Metall. Mater. Trans. A 33 (2002) 1373.
[31] K. Wang, N.R. Tao, G. Liu, J. Lu, K. Lu, Acta Mater. 54 (2006) 5281.